Surface Chemical Conversion of Organosilane Self-Assembled Monolayers with Active Oxygen Species Generated by Vacuum Ultraviolet Irradiation of Atmospheric Oxygen Molecules

Young-Jong KIM, Kyung-Hwang LEE*, Hikaru SANO, Jiwon HAN,

Takashi ICHII, Kuniaki MURASE, and Hiroyuki SUGIMURA[†]

Department of Materials Science and Engineering, Kyoto University,

Sakyo-ku, Kyoto 606-8501, Japan

*Present address: Research Institute of Industrial Science and Technology,

Maegok, Buk-gu, Ulsan 683-420, Korea

[†]E-mail address : hiroyuki.sugimura@ materials.mbox.media.kyoto-u.ac.jp

The chemical conversion of the top surface of *n*-octadecyltrimethoxy silane self-assembled monolayers (ODS-SAMs) on oxide-covered Si substrates using active oxygen species generated from atmospheric oxygen molecules irradiated with vacuum ultraviolet (VUV) light at 172 nm in

wavelength has been studied on the basis of water contact angle measurements, ellipsometry, X-ray photoelectron spectroscopy, and atomic force microscopy. An ODS-SAM whose water contact angle was 104° on average was prepared using chemical vapor deposition with substrate and vapor temperatures of 150 °C. The VUV treatment of an ODS-SAM sample was carried out by placing the sample in air and then irradiating the sample surface with a Xe-excimer lamp. The distance between the lamp and the sample was regulated so that the VUV light emitted from the lamp was almost entirely absorbed by atmospheric oxygen molecules to generate active oxygen species, such as ozone and atomic oxygen before reaching the sample surface. Hence, the surface chemical conversion of the ODS-SAM was primarily promoted through chemical reactions with the active oxygen species. Photochemical changes in the ODS-SAM were found to be the generation of polar functional groups, such as –COOH, –CHO, and –OH, on the surface and the subsequent etching of the monolayer. Irradiation parameters, such as

irradiation time, were optimized to achieve a better functionalization of the SAM top surface while minimizing the etching depth of the ODS-SAM. The ability to graft another SAM onto the modified ODS-SAM bearing polar functional groups was demonstrated by the formation of alkylsilane bilayers.

KEYWORDS: self-assembled monolayer (SAM), surface chemical conversion, vacuum ultraviolet (VUV) light, ozone, atomic oxygen, X-ray photoelectron spectroscopy (XPS)

1. Introduction

Organosilane self-assembled monolayers (SAMs) are expected to be used as high-resolution resist films because they provide a compact ultrathin layer. In addition, organosilane SAMs are of particular interest in a variety of applications, for example, corrosion protection,[1] microfluidics,[2,3] protein adsorption,[4] chromatography,[5] chemical

sensors,[6,7] and molecular electronics.[8-11] Organosilane films produced by self-assembly offer the great advantage of structural stabilization via multiple covalent and hydrogen bonds.[12] In contrast, self-assembled multilayers are expected to have functionalities that are not present in monolayers. For example, it is inferred that, owing to their in-plane molecular mobility, silane films might have the ability to self-heal to prevent structural defects in individual layers in a multilayer structure. These extremely robust and versatile materials are therefore remarkable candidates for the design of complex molecular architecture that might have a large impact on future nanotechnologies.[12-14]

Such multilayers have been formed through a layer-by-layer self-assembly process, which can usually be carried out using one of two methods. One method is the forming of a SAM on a SAM that has active functional terminal groups.[15-19] In the other method, the top surface, *i.e.*, the terminal groups, of the first SAM, are modified before the formation of the second SAM;[20-22] here, SAMs are reformed through various types of

irradiation, such as UV-light,[23,24] X-ray,[25,26] electron,[20,27,28] and plasma irradiation.[29-31] Howevers, the surface modification of organosilane SAMs has hardly been studied.

In our previous paper,[21,22] we investigated the vacuum ultraviolet (VUV) photodegradation of alkyl monolayers in the presence of atmospheric oxygen molecules. Here, VUV light of 172 nm in wavelength excites atmospheric oxygen molecules, resulting in the generation of ozone molecules as well as oxygen atoms in singlet and triplet states [O(1D) and O(3P), respectively], as described in the following equation.[32]

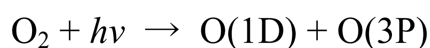

$$O_2 + h\nu \rightarrow O(1D) + O(3P)$$

Since these active oxygen species, particularly O(1D), have strong oxidative reactivity, the surface terminating $-CH_3$ groups on the monolayer are oxidized to polar functional groups, such as –COOH and –CHO. However, in the previous studies, the sample surface was directly irradiated with VUV light while the sample surface was exposed to active

oxygen species. Therefore, in addition to the oxidation of the SAM with the active oxygen, a VUV excitation of the alkylsilane SAM might be induced. Questions have remained concerning the exact roles of VUV light and active oxygen species.

In the present study, VUV light and VUV-light-generated active oxygen species were used to chemically introduce polar functional groups on the surface of alkylsilane SAMs. For the VUV irradiation of these SAMs, we have employed a particular set up, in which VUV light did not directly irradiate the SAM surface. Consequently, only the VUV-light-generated active oxygen participated in the oxidation of the SAMs, as schematically illustrated in Fig. 1. Furthermore, we attempted to stack another organosilane SAM on the VUV-light-treated SAMs using the silane coupling method,[33-37] in which the introduced functional groups work as reaction sites.

2. Experimental Procedure

The *n*-octadecyltrimethoxysilane self-assembled monolayers (ODS-SAMs) were prepared on silicon (Si) substrates by chemical vapor deposition.[38] Si(100) substrates (phosphorus-doped n-type wafers with a resistivity in the range of 1-10 Ω cm) covered with a native thin oxide layer (ca. 2 nm) were cleaned using a UV/ozone cleaning method[39] and hydroxylated simultaneously. Carboneous contamination was removed and consequently, the substrate surfaces became hydrophilic with a water contact angle of almost 0˚ so as to be terminated with hydroxyl (OH) groups. The cleaned and –OH terminated silicon substrates were placed together with a glass cup containing *n*-octadecyltrimethoxysilane [ODS; $CH_3(CH_2)_{17}Si(OCH_3)_3$, Gelest Inc.] liquid into a Teflon container with a volume of 120 cm^3. The container was tightly sealed with a screw cap and heated in an oven kept at 150 ˚C. Under this condition, the ODS liquid in the container vaporized and reacted with the OH groups on the substrate surface. The molecules were immobilized onto the substrate surface and also connected to adjacent ODS molecules through siloxane bridges. The

reaction time for SAM formation was fixed at 3 h. ODS-SAM formation was confirmed by the increase in the contact angle from 0 to 104° on average, and the thickness estimated by ellipsometry was about 1.5 nm. Detailed properties of the vapor-phase grown ODS-SAMs have already been reported.[40,41]

The VUV-light-exposure apparatus for ODS-SAM-coated samples is illustrated in Fig. 2. We used an excimer lamp as a source of VUV light at a wavelength of 172 nm (Ushio., UER20-172V; intensity at the lamp window, 10 mW cm^{-2}) as a light source. In our VUV-light-exposure system, the chamber was filled with ambient air, and the distance between the lamp window and the sample surface was fixed at 30 mm. The optical absorption coefficient at 172 nm in wavelength was reported to be in the range of 10 - 15 cm^{-1} atm^{-1} (at a partial pressure of 0.2 atm, namely, in ambient air).[41] The transmittance of 172 nm light through a 10 mm-thick air layer was calculated to be in the range of 5 - 13%. Its experimental value was about 10%, according to our

measurement. Consequently, the transmittance at 172 nm though an air layer of 30 mm is estimated to be less than 0.1%. At a distance of 30 mm, VUV light was concluded to be absorbed almost completely by atmospheric oxygen molecules, which are converted to active oxygen species such as ozone and atomic oxygen. The light intensity at the sample surface was calculated to be less than 0.010 mW cm^{-2}. No substantial amount of VUV light reached the sample surface. Hence, the direct irradiation of ODS-SAMs with VUV photons can't be expected in the present system. Only the VUV-light-generated active oxygen can participate in the surface modification of the ODS-SAMs. After VUV-light treatment, we attempted to stack another ODS-SAM using a similar silane coupling method, in which the oxidized SAM surface terminal groups acted as reaction sites.

The samples were characterized using a contact angle meter (Kyowa Interface Science., CA-X), and by ellipsometry (Otsuka Electronics., FE-5000), X-ray photoelectron spectrometery (XPS; Kratos

Analytical., ESCA-3400), and atomic force microscopy (AFM; SII Nanotechnology., SPA-300HV + SPI-3800N). The static water contact angles of the sample surfaces were measured in an atmospheric environment. SAM thickness was measured by ellipsometry. The chemical bonding states of each sample were examined by XPS using a Mg Kα X-ray source of 10 mA and 10 kV. The morphology and surface roughness of the samples were measured by AFM.

3. Results and Discussion

Figure 3 shows that both the water contact angles and film thicknesses of the *n*-octadecyltrimethoxysilane self-assembled monolayers (ODS-SAMs) decreased monotonically with an increase in irradiation time. The decrease in the water contact angle is due to the progressive introduction of polar functional groups onto the monolayer surface toward a VUV-irradiation time of 900 s. After 900 s, the contact angle settled at zero, indicating that the polar functional groups were also completely

removed from the surface. Here, we can divide the changes in water contact angle and thickness into three regions labeled [a], [b], and [c] in Fig. 3. In region [a], the water contact angle decreased rapidly, whereas in region [b] it maintained intermediate values at approximately 31 - 44˚. In region [c], it continued to decrease, approaching 0°. Although the decreasing rate in region [c] is almost identical to that in region [b], these regions can be clearly separated from the results, as shown in Fig. 3(b). The thickness gradually decreased in regions [a] and [b], and its decreasing rate became more rapid at the boundary of regions [b] and [c]. Finally, the water contact angle remained at approximately 0˚. The concomitant change in film thickness also indicated that the ODS-SAM is gradually removed by VUV-light-generated active oxygen. As can be understood from Fig. 2 that a monolayer of siloxane remained on the substrate even when all organic parts are degraded from the ODS-SAM. The thickness estimated by ellipsometry was 0.2 - 0.4 nm, as shown in Fig. 3(b).

This VUV-irradiated surface chemical conversion of ODS-SAMs was studied in more detail using XPS. Figure 4 shows the C 1s and Si 2p XPS spectra of ODS-SAM samples prior to and after VUV irradiation for 200, 400, 900, and 1500 s. By VUV irradiation for 200, 400, 900, and 1500 s, the amount of carbon on the sample decreased, whereas the amount of silicon on the sample increased. The C 1s peak of VUV-irradiated ODS-SAMs can be deconvoluted into four components centered at 285.0, 286.1, 287.4, and 288.7 eV, as demonstrated in Fig. 5. The later three components correspond to C–O, C=O, and COO components, respectively, while the first component is a C–C component. Thus, it was shown that polar functional groups containing oxygen, that is, the origin of the hydrophilicity in this sample, are formed by the VUV-light treatment; therefore, XPS results as a function of VUV-irradiation time also indicate progressive functionalization, as confirmed by water contact angle measurements. Note that the intensities of the C 1s peaks for 900 and 1500 s are almost the same. This indicates

that these peaks are due to contamination, that is, atmospheric impurities stuck on the sample, as is often the case with the XPS of samples transferred in ambient atmosphere. Therefore, also from the XPS spectra, we considered that the monolayer is almost decomposed at an irradiation time of 900 s, as indicated by the contact angle measurement. The spectrum of the ODS-SAM sample irradiated for 400 s, that is, region [b], showed characteristic features. A distinctive feature appeared in the range of approximately 286−289 eV in the C 1s XPS spectra, as indicated in Fig. 4(a), which corresponded to oxidized organic components, *i.e.,* those originating from polar functional groups (OH, CHO, and COOH). From the deconvolution of this spectrum (Fig. 5), we confirmed that the concentration of the C–C component decreased, while those of the oxydized components increased, compared with the values for unirradiated ODS-SAMs. The C 1s atomic percentage data summarized in Table I show progressive increases in the surface densities of polar functional groups (detected as C–O, C=O, and COO components) with

VUV-light irradiation until 400 s; however, for longer VUV-light irradiation times, there was a decrease in their percentages. We have tried to confirm the presence of OH, CHO and COOH on the sample surfaces based on infrared (IR) spectroscopy as well. However, we could obtain no IR spectra with a sufficient signal-to-noise ratio both in attenuated total reflection and reflection absorption spectroscopy methods, because of the background noise due to water vapor and the low IR reflectivity of Si substrates. As a consequence, we can consider that the monolayer after a VUV-light treatment of 400 s maintains the largest number of polar functional groups on the surface.

The surface structure of the VUV-light-treated monolayer was monitored using AFM. Topography images (Fig. 6) indicate that VUV-light treatments of 200, 400, and 900 s do not significantly alter the initial surface structure of the monolayer. RMS roughnesses were all approximately 0.1 nm. The oxidation and etching of the ODS-SAMs using VUV-light-generated active oxygen was found to proceed

uniformly.

The chemical changes induced on the ODS-SAMs by the VUV-light irradiation under the experimental conditions in this paper are considered to be primarily due to the VUV-light-generated active oxygen, since there was no substantial VUV light intensity reaching the sample surface, as explained in the experimental section. The VUV light intensity at the sample surfaces was less than 0.010 mW cm^{-2}. This very low intensity VUV light might cause a small number of chemical changes in the ODS-SAMs if the irradiation is prolonged for 200 – 500 s. We have estimated the packing density of our vapor-phase-grown ODS-SAM to be in the range of 7×10^{13} - 8×10^{13} ODS molecules cm^{-2} from the occupied area of one ODS molecule, which we reported to be 1.2 - 1.5 nm^2/molecule.[39] When irradiated for 100 s at an intensity of 0.010 mW cm^{-2} with photons of 7.2 eV, *i.e.*, the photon energy of 172 nm light, the total photon flux becomes 9×10^{14} cm^{-2}, corresponding to approximately 10 photons per ODS molecule. This number might not be negligible. On

the other hand, the VUV absorption edge of polyethylene (PE), that is, a saturated hydrocarbon similar to ODS, is known to be about 160 nm.[42) In order to dissociate C-C and C-H bonds in PE, VUV light with a wavelength shorter than this absorption edge wavelength is required.[43) Indeed, it has been reported that under a high vacuum condition on the order of 10^{-4} Pa no chemical change was induced on a PE substrate by VUV irradiation at 172 nm, while the substrate was etched with irradiation at 124 or 146 nm.[44) Thus, VUV light at 172 nm is expected to hardly be absorbed by ODS-SAMs, that consist of saturated hydrocarbon molecules.[45) We have also confirmed that no apparent change was recognized in the ODS-SAMs by VUV irradiation at 172 nm in vacuum. Therefore, we conclude that such a small number of photons, that is, tens of photons per molecule, had almost no effect on the chemical changes of the ODS-SAMs.

In order to prove the ability to graft another set of organic compounds onto the VUV-light-functionalized SAM, a second layer of

ODS molecules was grafted. The evolution of the surface conversion was studied by measuring the water contact angle and film thickness (Fig. 7). The presence of polar functional groups on the modified surface should allow the grafting of alkylsilane molecules. Indeed, as shown in Fig. 7(a), the deposition of the second ODS-SAM onto the ODS-SAM/Si substrate modified with the VUV-generated active oxygen was possible for all the VUV treatment times, and the water contact angles of the second layer of the ODS-SAM substrates reached 100° on average. The primary chemistry behind this second layer deposition is most likely hydrogen bonding between hydrolyzed ODS molecules consisting of the second layer and the polar functional groups on the first modified layer surface. It is plausible that silane coupling reactions proceed further and that some of the hydrogen bonds are converted to Si-O-C bonds. As clearly demonstrated in Fig. 7(b), however, the thickness of the films grown on VUV-light-treated ODS-SAM substrates increased until 400 s and decreased after 400 s until a treatment time of 1200 s, and then a

plateau was observed at an average of 1.5 nm. A film of 2.8 nm thickness on average was grown with a VUV-light-treatment time of 400 s; therefore, we considered that 400 s was the most suitable VUV-light-treatment time as an optimum condition. Under this condition, we can attain a maximum density for the polar functional groups, which serve as sites for second monolayer growth, and minimize the loss of the thickness of the first monolayer due to etching.

4. Conclusions

The surface chemical conversion of *n*-octadecyltrimethoxysilane self-assembled monolayers (ODS-SAMs) with active oxygen species generated by the VUV-light excitation of atmospheric oxygen molecules has been investigated by water contact angle analysis, film thickness analysis, XPS, and AFM. In the VUV-light treatment experiments, an ODS-SAM sample placed in air was irradiated with a Xe excimer lamp located 30 mm above the sample surface. At this distance, the VUV light

emitted from the lamp was almost completely absorbed by atmospheric oxygen molecules, which were converted to active oxygen species such as ozone and atomic oxygen. Finally, the VUV light intensity at the sample surface was attenuated to less than 0.1% of the initial intensity at the lamp window. Hence, the ODS-SAM surface was not substantially irradiated with VUV light in our experimental set up. Since all the VUV light was adsorbed by oxygen molecules in the space above the sample and was consumed to generate active oxygen, the primary photochemical reaction proceeding on the ODS-SAM was its oxidation with the VUV-light-generated active oxygen. Polar functional groups such as –COOH, –CHO, and –OH were consequently formed on the sample surface. When the VUV-light treatment was further prolonged, the ODS-SAM was gradually etched and all of its alkyl region was removed completely in the end. We have also demonstrated that the oxidized groups served as reaction sites for immobilizing additional organosilane molecules. For bilayer fabrication, we have optimized conditions of the

VUV-light treatment by which maximum polar functional group density the minimum etching depth were attainable. This method will be applicable to the fabrication of multilayers consisting of a variety of organosilane molecules. In addition, our investigation helps to clarify the role of active oxygen in the photoreactivity of SAMs.

1) P. E. Laibinis and G. M. Whitesides: J. Am. Chem. Soc. **114** (1992) 9022.
2) B. Zhao, J. S. Moore, and D. J. Beebe: Science **291** (2001) 1023.
3) Y. Feng, Z. Zhou, X. Ye, and J. Xiong: Sens. Actuators A. **108** (2003) 138.
4) P. Ying, G. Jin, and Z. Tao: Colloids Surf. B **33** (2004) 259.
5) M. J. Wirth, R. W. P. Fairbank, and H. O. Fatunmbi: Science **275** (1997) 44.
6) Y. Cui, Q. Wei, H. Park, and C. M. Lieber: Science **293** (2001) 1289.
7) D. Niwa, T. Homma, and T. Osaka: Jpn. J. Appl. Phys. **43** (2004)

L105.

8) J. Collet, M. Bonnier, O. Bouloussa, F. Rondelez, and D. Vuillaume: Microelectron. Eng. **36** (1997) 119.

9) S. Lenfant, C. Krzeminski, C. Delerue, G. Allan, and D. Vuillaume: Nano Lett. **6** (2003) 741.

10) S. Kobayashi, T. Nishikawa, T. Takenobu, S. Mori, T. Shimoda, T. Mitani, H. Shimotani, N. Yoshimoto, S. Ogawa, and Y. Iwasa: Nat. Mater. **3** (2004) 317.

11) M. Halik, H. Klauk, U. Zschieschang, G. Schmid, C. Dehm, M. Schütz, S. Maisch, F. Effenberger, M. Brunnbauer. and F. Stellacci: Nature **431** (2004) 963.

12) A. Baptiste, A. Gibaud, J. F. Bardeau, K. Wen, R. Maoz, J. Sagiv. and B. M. Ocko: Langmuir **18** (2002) 3916.

13) R. Maoz, E. Frydman, S. R. Cohen, and J. Sagiv: Adv. Mater. **12** (2000) 725.

14) R. Maoz, S. R. Cohen, and J. Sagiv: Adv. Mater. **11** (1999) 55.

15) R. Buller, H. Cohen, T. R. Jensen, K. Kjaer, M. Lahav, and L. Leiserowitz: J. Phys. Chem. B **105** (2001) 11447.

16) I. Weissbuch, S. Guo, R. Edgar, S. Cohen, P. Howes, K. Kjaer, J. Als-Nielsen, M. Lahav, and L. Leiserowitz: Adv. Mater. **10** (1998) 117.

17) H. Yonezawa, K. H. Lee, K. Murase, and H. Sugimura: Chem. Lett. **35** (2006) 12.

18) A. Hatzor, T. van der Boom-Moav, S. Yoshelis, A. Vaskevich, A. Shanzer. and I. Rubinstein: Langmuir **16** (2000) 4420.

19) J. A. Libera, R. W. Gurney, S. T. Nguyen, J. T. Hupp, C. Liu, R. Conley, and M. J. Bedzyk: Langmuir **20** (2004) 8022.

20) K. Ogawa, N. Mino, H. Tamura, and M. Hatada: Langmuir **6** (1990) 851.

21) L. Hong, H. Sugimura, T. Furukawa, and O. Takai: Langmuir **19** (2003) 1966.

22) H. Sugimura, L. Hong, and K. H. Lee: Jpn. J. Appl. Phys. **44** (2005)

5185.

23) S. V. Roberson, A. J. Fahey, A. Sehgal, and A. Karim: Appl. Surf. Sci. **200** (2002) 150.

24) T. Ye, D. Wynn, R. Dudek, and E. Borguet: Langmuir **17** (2001) 4497.

25) S. R. Wasserman, G. M. Whitesides, I. M. Tidswell, B. M. Ocko, P. S. Pershan, and J. D. Axe: J. Am. Chem. Soc. **111** (1989) 5852.

26) T. K. Kim, X. M. Yang, R. D. Peters, B. H. Sohn, and P. F. Nealey: J. Phys. Chem. B **104** (2000) 7403.

27) S. Hou, Z. Li, Q. Li, and Z. F. Liu: Appl. Surf. Sci. **222** (2004) 338.

28) J. Park and H. Lee: Mater. Sci. Eng. C **24** (2004) 311.

29) J. -D. Liao, M. -C. Wang, C. -C. Weng, R. Klauser, S. Frey, M. Zharnikov, and M. Grunze: J. Phys. Chem. B **106** (2002) 77.

30) M. Tatoulian, O. Bouloussa, F. Moriere, F. Arefi-Konsari, J. Amouroux, and F. Rondelez: Langmuir **20** (2004) 10481.

31) C. -C. Weng, J. -D. Liao, Y. -T. Wu, M. -C. Wang, R. Klauser, M.

Grunze, and M. Zharnikov: Langmuir **20** (2004) 10093.

32) R. P. Roland, M. Bolle, and R. W. Anderson: Chem. Mater. **13** (2001) 2493.

33) S. L. Brandow, M. -S. Chen, R. Aggarwal, C. S. Dulcey, J. M. Calvert, and W. J. Dressick: Langmuir **15** (1999) 5429.

34) N. Ichinose, H. Sugimura, T. Uchida, N. Shimo, and H. Masuhara: Chem. Lett. (1993) 1961.

35) B. Lee and N. A. Clark: Langmuir **14** (1998) 5495.

36) H. Sugimura and N. Nakagiri: Appl. Phys. A **66** (1998) S427.

37) H. Sugimura, K. Ushiyama, A. Hozumi, and O. Takai: Langmuir **16** (2000), 885.

38) H. Sugimura, A. Hozumi, T. Kameyama, and O. Takai: Surf. Interface Anal. **34** (2002) 550.

39) K. Hayashi, N. Saito, H. Sugimura, O. Takai, and N. Nakagiri: Langmuir **18** (2002) 7469.

40) H. Sugimura and N. Nakagiti: J. Photoplym. Sci. Technol. **10** (1997)

661.

41) K. Watanabe, E. C. Y. Inn, and M. Zelikoff: J. Chem. Phys. **21** (1953) 1028.

42) S. Onari: J. Phys. Soc. Jpn. **26** (1969) 500.

43) R. A. George, D. H. Martin, and E. G. Wilson: J. Phys. C **5** (1972) 871.

44) F. Truica-Marasescu and M. R. Wertheimer: Macromol. Chem. Phys. **206** (2005) 744.

45) At 172 nm, the optical transparency of a PE film with a thickness in the range of 1 - 2 nm is greater than 99.99%, similarly to ODS-SAM, as estimated from the optical densities of PE reported in R. H. Partridge: J. Chem. Phys. **45** (1966) 1685.

Fig. 1. Schematic illustration of layer-by-layer chemical self-assembly of ODS/(oxidized ODS)/Si films, where oxidized ODS means ODS-SAM treated with VUV-light-generated active oxygen in order to convert terminal methyl groups to active groups such as carboxyl group.

Fig. 2. Schematic illustration of VUV-irradiation apparatus.

Fig. 3. Changes in (a) water contact angles and (b) thickness of ODS-SAM with irradiation time of VUV light.

Fig. 4. (a) C 1s and (b) Si 2p XPS spectra of ODS-SAM surfaces before and after irradiation with VUV light for 200-1500 s.

Fig. 5. Deconvolved C 1s XPS spectrum of ODS-SAM surface that underwent VUV irradiation for 400 s.

Fig. 6. AFM topography images and RMS roughnesses of ODS-SAM surfaces prepared using four different VUV-light treatment times (tapping mode; image size, 500×500 nm^2).

Fig. 7. Changes in (a) water contact angles and (b) thicknesses of ODS bilayer with irradiation time of VUV light.

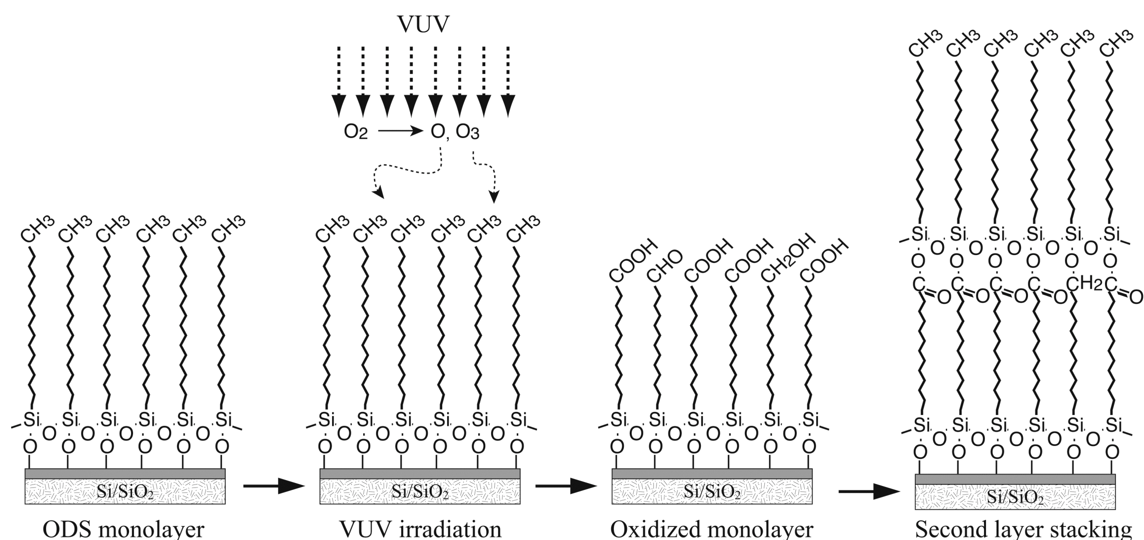

Fig. 1. Schematic illustration of layer-by-layer chemical self-assembly of ODS/(oxidized ODS)/Si films, where oxidized ODS means ODS-SAM treated with VUV-light-generated active oxygen in order to convert terminal methyl groups to active groups such as carboxyl group.

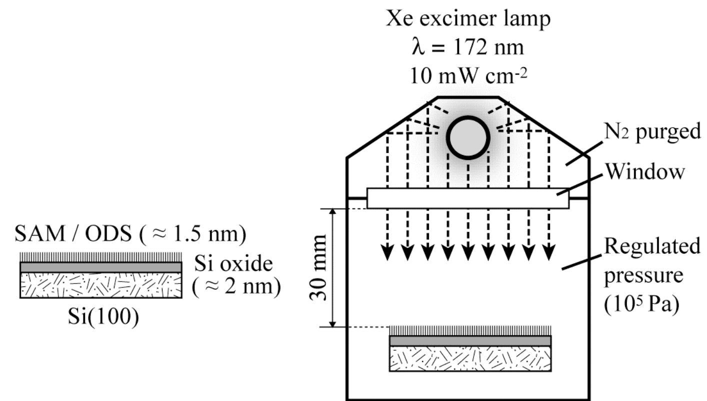

Fig. 2. Schematic illustration of VUV-irradiation apparatus.

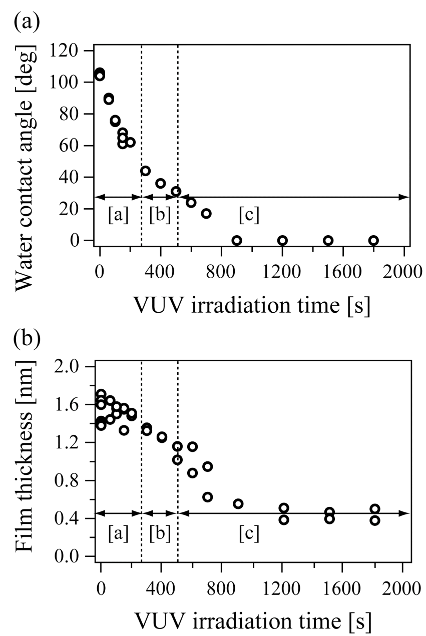

Fig. 3. Changes in (a) water contact angles and (b) thickness of ODS-SAM with irradiation time of VUV light.

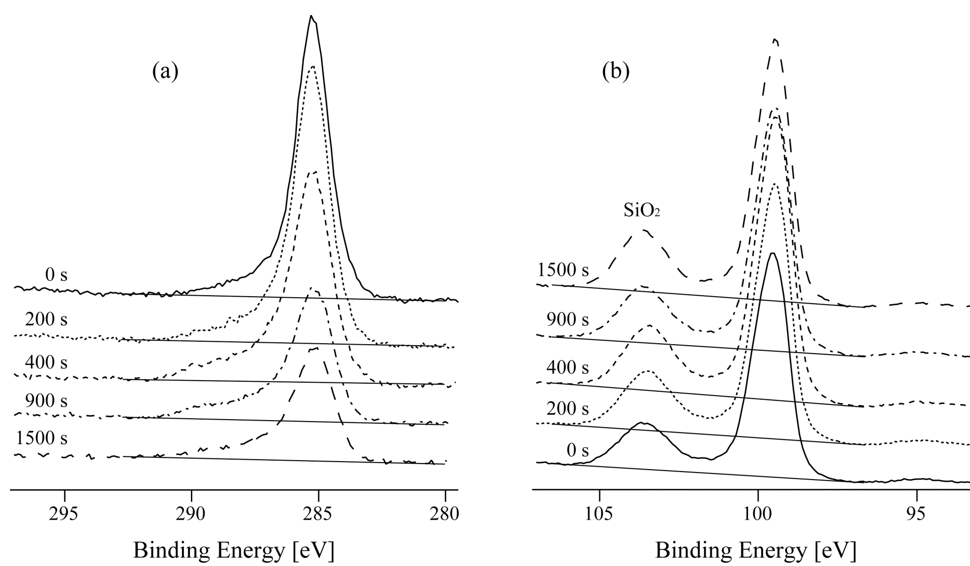

Fig. 4. (a) C 1s and (b) Si 2p XPS spectra of ODS-SAM surfaces before and after irradiation with VUV light for 200-1500 s.

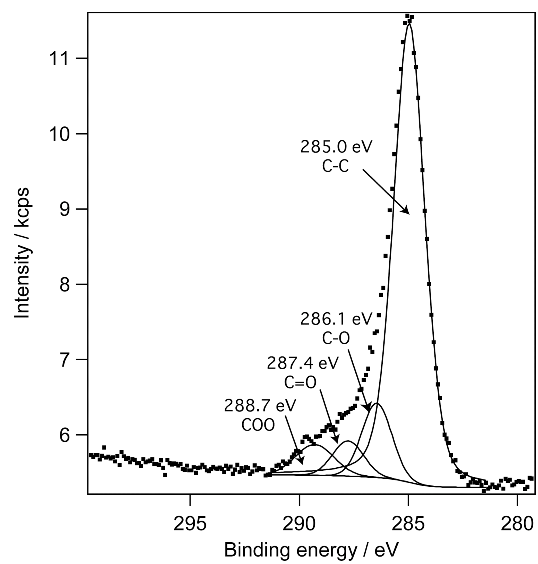

Fig. 5. Deconvolved C 1s XPS spectrum of ODS-SAM surface that underwent VUV irradiation for 400 s.

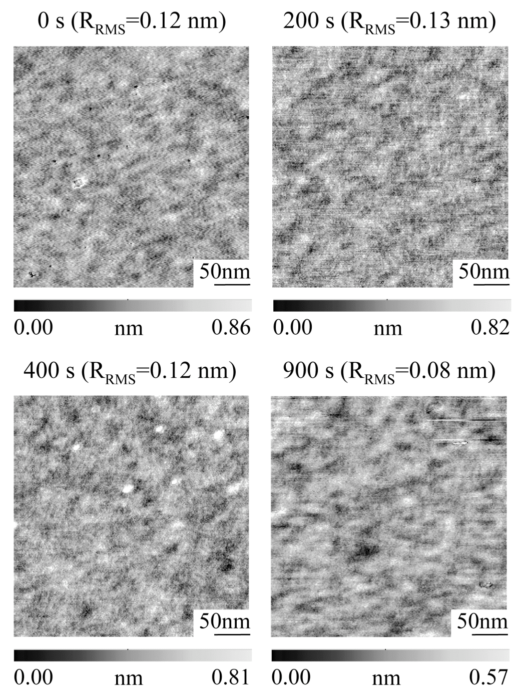

Fig. 6. AFM topography images and RMS roughnesses of ODS-SAM surfaces prepared using four different VUV-light treatment times (tapping mode; image size, 500×500 nm^2).

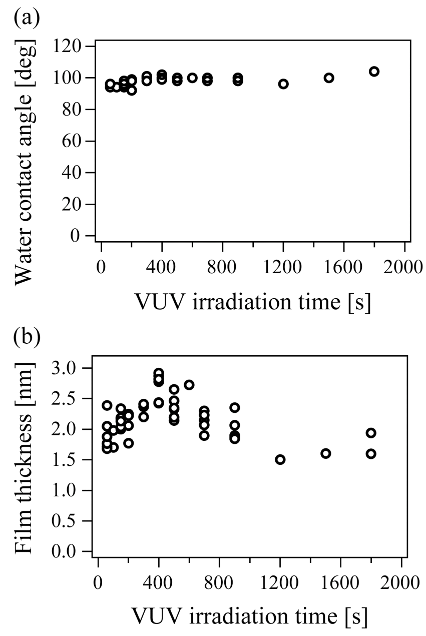

Fig. 7. Changes in (a) water contact angles and (b) thicknesses of ODS bilayer with irradiation time of VUV light.

Table Ⅰ. Atomic percentages of four elements including C 1s of different carbon moieties determined by XPS versus VUV-light treatment time.

VUV-light treatment time [s]	Si [%]	C [%]				O [%]	C/O
		C-C [%]	C-O [%]	C=O [%]	COO [%]		
0	40	25	5	2	1	27	1.2
200	40	20	5	2	2	31	0.9
400	40	15	6	1	3	35	0.7
900	43	14	3	1	2	37	0.6